HEAT AND MASS TRANSFER 97

Proceedings of the Third ISHMT-ASME Heat and Mass Transfer Conference, and Fourteenth National Heat and Mass transfer Conference

December 29-31, 1997

INDIAN INSTITUTE OF TECHNOLOGY KANPUR

Editors

G. BISWAS
S. SRINIVASA MURTHY
K. MURALIDHAR
V.K. DHIR

In Cooperation with Coordinating Scientists

G.A. Dreitser, Russia
R.K. Shah, USA
F. Arinc, Turkey
N.K. Mitra, Germany
V.V. Wadekar, United Kingdom
K. Suzuki, Japan
A.T. Prata, Brazil
C.V. Madhusudana, Australia

Organised under the Auspices of the

INDIAN SOCIETY FOR HEAT AND MASS TRANSFER

In Cooperation with the

AMERICAN SOCIETY OF MECHANICAL ENGINEERS

Narosa Publishing House
New Delhi Mumbai Madras Calcutta London

ED_AK_CC.pdf

Determination of Optimal Row Spacing for a Staggered Pin Fin Array in a Turbine Blade Cooling Passage

E.E. Donahoo, A.K. Kulkarni, A.D. Belegundu and C. Camci*
Department of Mechanical Engineering, *Department of Aerospace Engineering,
The Pennsylvania State University, University Park PA 16802, USA

ABSTRACT

Pin fin configurations are of interest in turbine blade design due to the enhanced cooling they provide. In addition, pin fins which extend from the walls of hollow blades provide structural integrity and stiffness to the blade itself. Numerous pin fin shapes and arrangements are possible, but only certain combinations offer high heat transfer capability while maintaining low overall total pressure loss. This study presents results from 2-D numerical simulations of coolant airflow through a turbine blade internal cooling passage. The simulations model viscous flow and heat transfer over circular fins in a staggered arrangement of varying pin spacing. Preliminary analysis over a wide range of Reynolds numbers indicates existence of an optimal spacing for which maximum heat transfer and minimum total pressure drop occurs. Pareto plots, which graphically identify the optimum data points with multiple optimization parameters, were obtained for a range of Reynolds numbers and fin spacings in a staggered pin fin arrangement. There is a steady increase in pin fin heat transfer up to a certain number of rows, then a gradual decrease in heat transfer in subsequent rows. Knowledge obtained from such findings can be used to determine the number of pin fins used, as well as the ultimate fin arrangement.

INTRODUCTION

Strenuous demands are put on gas turbine blades operating in modern engines. Improvements in engine performance are closely related to increases in the tolerance level of turbine inlet temperatures. The ability to operate at increasingly high temperatures has been a result of both improvements in materials capability to endure high thermal loads and advances in cooling schemes for hot section components. Air-cooled turbine blades have made high cycle temperatures possible, resulting in high specific power. In the immediate future, it is most likely that air-cooled turbine blades will continue to be the solution for handling the higher turbine inlet temperatures with optimization of the design being necessary.

Recently, pin fins have been used in the turbine blade flow channels in order to enhance its cooling characteristics as illustrated in figure 1. The pin fin itself is a cylindrical rod extending from the passage walls, and such pin fins are predominantly located near the blade's trailing edge. These fins affect the coolant flow negotiating around them in three ways: i) they increase the total heat transfer surface area within the passage, thus leading to increased convection heat transfer; ii) their staggered arrangement forces coolant air to travel a more tumultuous path, increasing the turbulence level of the flow,

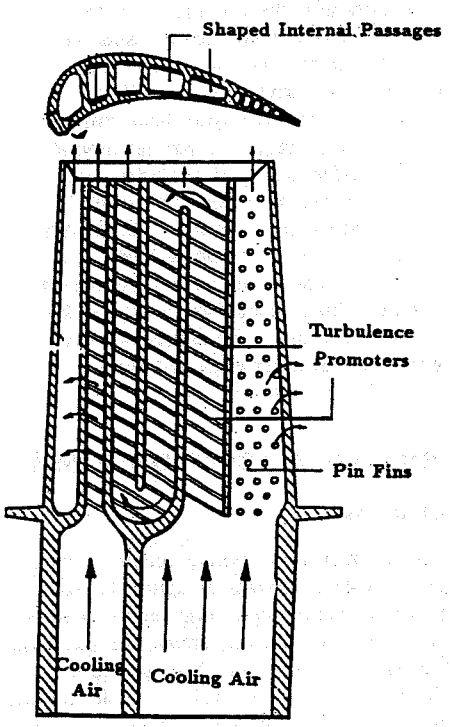

Figure 1: Turbine blade internal cooling passage [Zhang et al.,1993].

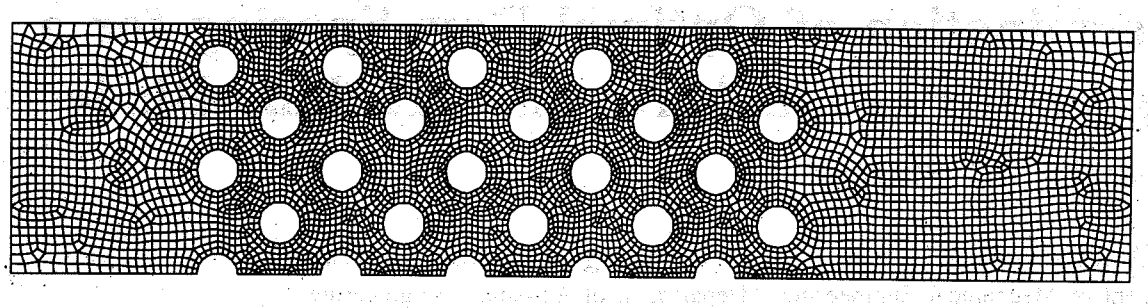

Figure 2. Computational domain of cooling passage with numerical mesh

resulting in greater convection cooling, and iii) the presence of fins also presents added blockage to the flow, introducing a total pressure loss to the flow, which is undesirable for a given pressure head available from the compressor. Hence, the design of a pin fin arrangement requires optimization of certain parameters to ensure both desirable heat transfer and acceptable total pressure losses.

Previous studies have shown that logitudinal pin spacing indeed affects the overall heat transfer characteristics and total pressure drop. Peng[1] conducted studies on cross pins, which extend the full height of the channel, and pin fins that extend only partially into the channel. He found experimental values for the heat transfer coefficient using the Colbourn factor and concluded that fin spacing affects partial pin fins slightly more than cross pins. Armstrong and Winstanley[2] reviewed studies on local and array-averaged heat transfer in converging flow channels with a staggered pin alignment, and found that pin fin heat transfer averaged over the array appears to vary with Reynolds number to a power between 0.6 and 0.7, depending on pin height-to-diameter ratio, H/D. Effectiveness of pin fin arrays has also been studied by Metzger et al.[5], Van Fossen[7] and Chyu[9]. The objective of the present study is to derive an optimum fin spacing based on the detailed computation of heat flux and total pressure drop that can later be used in the design of fin arrangements and shape.

MODEL OF BLADE FLOW PASSAGE

Physical Model

Highly sophisticated cooling schemes employing complex passageway designs (shown in figure 1) have been used to maintain turbine blades operating under extreme conditions to stay within tolerable thermal limits. In this study, the domain itself consists of 10 rows of staggered circular pin fins (shown in figure 2) within the turbine blade cooling passage. Figure 2 shows the element mesh using an unstructured grid of the cooling passage. Only one-half the passage is modelled due to symmetry. The top and bottom planes represent the channel wall and a symmetry plane respectively.

Mathematical model

This current study uses a general purpose visous flow solver to simulate the flow and heat transfer inside the turbine blade passage (see FIDAP[10]). Using the Galerkin finite element procedure to the stationary Navier-Stokes equations, a set of nonlinear algebraic equations is obtained and represented in matrix form as:

$$K(u) = F \tag{1}$$

where K is the global matrix system, u is the global vector of unknowns (velocities, pressures, and temperatures) and F is a vector which includes the effects of body forces and boundary conditions. The numerical simulations of the flowfield inside a turbine blade passage involves solving the momentum and energy equations. In this problem, the momentum equation does not strongly depend on the temperature field, and is thus considered a weakly coupled problem. In such flows, the momentum equation can be solved independently of the other scalar equations, followed by the solution of the energy equation with a known velocity field. A two-equation $k-\varepsilon$ turbulence model is employed to represent the turbulent eddies and vortex mixing associated with flow through a pin fin array.

The computational domain modelling the turbine blade flow passage consists of an inlet, outlet, wall, and symmetry plane. The flowfield in the streamwise direction is assumed to be symmetric about the centerline, so only one-half the passage is modelled. At the inlet, uniform velocity ($U^* = U/U_i = 1$) and uniform temperature ($T^* = (T - T_i)/(T_s - T_i) = 0$ for coolant flow) profiles were given. Along the wall boundaries, the no slip boundary condition was imposed for velocity, while a constant profile ($T^* = 1$ for hot walls) was imposed for temperature. In wall-bounded turbulent flows, the near wall modelling methodology was invoked using special near wall elements.

THE OPTIMIZATION PROBLEM

Finding a pin fin configuration design that yields both favorable heat transfer characteristics and total pressure drop can be considered an engineering problem of optimization. As with this particular study, different objectives may not be compatible; the variables that optimize one objective may be far from optimal for another. For example, variables affecting heat flux and total pressure drop include pin spacing, number of pins, pin size and shape, as well as passage curvature. Certain pin spacing may produce favorable cooling characteristics, which is one objective, but also produce unfavorable pressure drops which is another objective.

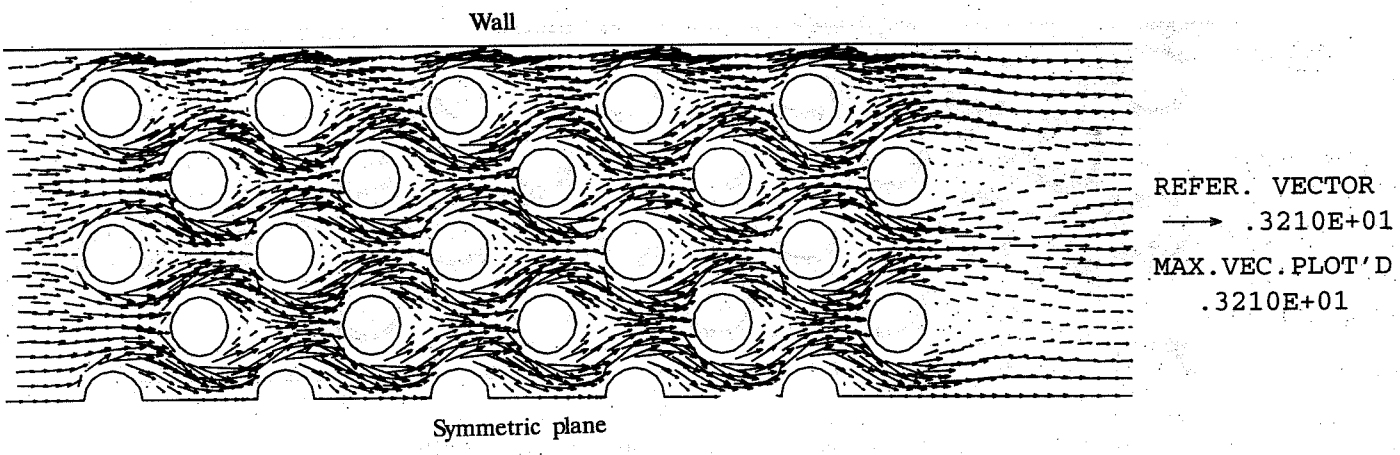

Figure 3a. Velocity vector plot (magnified 40%) for Re_D = 1270 and x/D = 1.5. Length of arrows indicate magnitude of velocity, which ranges from U^* = 0.357 to U^* = 3.21.

The approach taken was to generate a set of feasible designs, and then select an optimal design based on heat flux and total pressure drop. The variable in this study is the longitudinal pin spacing, x, which is the distance between centers of two adjacent pins in the streamwise direction. Different pin spacings were modelled while holding all other design parameters constant (i.e., Re_D, inlet flow temperature, T_i, pin diameter, D = 0.01 m and transverse spacing, x_T); thus the sole effect is to isolate one design variable, that being x. The transverse spacing, x_T, was held to a constant value of $2.5D$. Fourteen values of (x/D) were investigated between 1.0 and 4.0. This was done for four values of Reynolds numbers: 1270, 3980, 7310, and 13800. The Reynolds numbers chosen were in conjunction with case studies used by Armstrong[2]. For flow regimes between $10^3 < Re_D < 10^5$, the boundary layers around the cylinders contain both laminar and turbulent regions; thus all case studies were modelled using a $k-\varepsilon$ turbulence model.

RESULTS AND DISCUSSION

Flow Characteristics

A velocity vector plot for Re_D = 1270 with x/D = 1.5 is shown in figure 3a. Coolant flow enters the turbine passage from the left and exits to the right to the ambient. All governing equations are nondimensionalized to provide a measure of the relative importance of various terms and identify dominant physical phenomena. Hence, the inlet velocity is scaled accordingly as $U^* = U/U_i$. For Re_D = 1270, this would correspond to an inlet velocity of U_i = 15.48 m/s. The scale identifies the relative magnitudes of the velocity vectors. As figure 3a illustrates coolant flow negotiating around the first row of fins, three distinct processes develop. First, as flow passes through the converging cross section presented by adjacent fins, a jet is formed, accelerating the flow to values approximately $1.5U^*$. Second, behind the fins, formation of wakes generates small but discernable recirculating zones of relatively low velocity. Although the recirculation zones in the wakes have low velocities, high strain rates promote relatively high turbulence. The third process develops in subsequent rows, where the staggered pin arrangement forces the jet generated from the previous row to negotiate around another set of fins; in so doing, secondary jets are formed in converging cross sections. This staggered alignment creates a jet-wake interaction, where the outer region of the wake is entrained with accelerating flow negotiating the next set of fins. The accelerating flows coalesce from both sides, spawning new jets of equal magnitude as ones formed from the first row. The dynamics of these jet-wake interactions have a significant effect on the overall flowfield behavior. It is also apparent that the greatest acceleration occurs near the walls, where velocity magnitudes reach $2.8U^*$. The interference of wakes and growth of boundary layers cause the near wall velocity values to increase from approximately $2.3U^*$ crossing row 1, to $2.5U^*$ in row plane 2, and finally to values of $2.8U^*$ in row plane 9.

Flows at Re_D = 3980, 7310, and 13800 respectively showed similar features (not presented here for brevity). At Re_D = 3980, the size of the wakes were uniform for pins within the core flow and stretched approximately 0.4 diameter. For pins adjacent to the wall, the average wake size was larger, around 0.5 diameter. This difference in size is most likely due to local accelerations near the wall which is greater than anywhere else in the flow, producing a higher local Reynolds number. Thus, the effect of near wall dynamics on heat transfer can have significant implications in pin fin design and arrangement.

Figure 3b is a temperature contour plot of the same coolant flow as shown in figure 3a. The coolant flow enters with a nondimensional inlet temperature of T^* = 0, while the hot walls and fin surfaces are at a uniform temperature of T^* = 1. The flow enters from the left, and encounters the first row of fins, where large temperature gradients near the pin surfaces appear, as denoted by contour levels A (described by the legend). It is here that the local heat flux is expected to

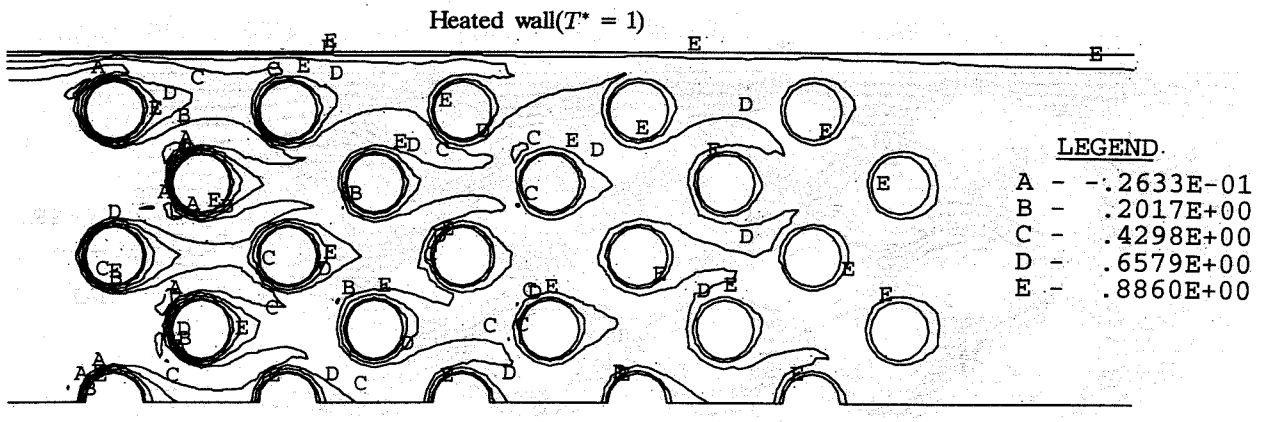

Figure 3b: Temperature contour plot (magnified 40%) for Re_D = 1270 and x/D = 1.5.

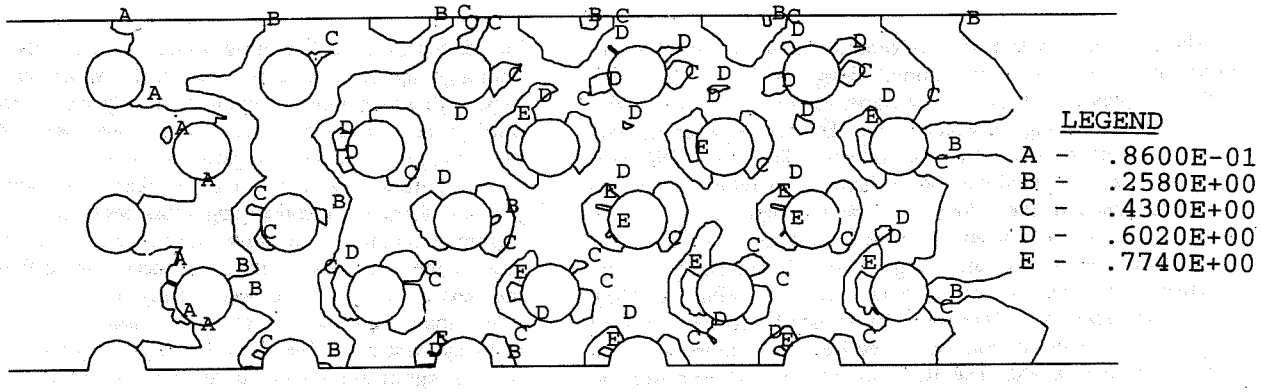

Figure 3c: Turbulent kinetic energy contour plot (magnified 40%) for Re_D = 1270 and x/D = 1.5.

be the highest. The wake is heated to about T^* = 0.37. The average core flow reaches a near uniform value by row 5, and increases steadily further from about T^* = 0.43 to T^* = 0.77. Note the large temperature gradients along the wall continue to be significant until row 7. Flow exiting to the ambient is approximately at T^* = 0.75, indicating subtantial heating of the coolant flow and substantial thermal energy gained from convection cooling of fin surfaces. Knowledge of the heat transfer characteristics can also be helpful in determining whether thermal stresses generated within the passage are within tolerable limits.

Figure 3c is a turbulent kinetic energy contour plot with Re_D = 1270 and x/D = 1.5. The flow enters with a freestream turbulence intensity of 1%, from which the freestream turbulent kinetic energy, k, defined as $IU_\infty/100$, is assigned a value of 0.0001. But by rows 3 and 4, vortex shedding and subsequent vortex interaction from adjacent wakes become substantial enough to produce appreciable levels in the turbulent kinetic energy. The most intense turbulent kinetic energy seems to be produced in the forward part of the fins in rows 6-10 where vortex stretching is strong. Favorable pressure gradients are responsible for the production of vorticity at a solid surface, while adverse pressure gradients act as a sink of vorticity. Hence, the peak turbulent kinetic energy contour levels may be a result of rapid vorticity production along the forward pin section that "breaks away", becoming unstable and leading to full scale turbulence by row 4 and 5.

Total Pressure Distributions

Figure 4 is a surface plot of the total pressure deviation with respect to p_{ref} = 100 kPa for Re_D = 1270 and x/D = 1.5. For an isothermal, frictionless flow, the total pressure would remain constant. However, for a viscous, turbulent flow, there will be losses due to friction. Mean kinetic energy level of the flow is reduced by the viscous dissipation mechanism. This reduction is many times measurable as total pressure loss.

As flow passes the last row of fins and exits the coolant passage, the total pressure levels off. The drop in the surface heights is a relative measure of the amount of pressure head lost within the passage. Minimizing this difference is vital in pin fin design. Similar features were found for other x/D ratios for the range of Reynolds numbers studied.

Pareto Curves

Pareto curves provide a graphical means of identifying optimum points having more than one objective function (the function to be maximized or minimized). Figure 5 is an illustration of a "generic" Pareto curve. The x and y axes correspond to the first and second objective functions (f_1 and f_2) to be optimized. If the goal is to maximize both parameters f_1 and f_2, maximizing one may not necessarily maximize the other. The key is finding the compromise between both functions that would lead to an optimum point for both functions. For example, point A obtains the maximum value of f_1, but it also renders a minimal value for f_2. Point C obtains the maximum value of f_2, but renders only the minimal value for f_1. The ideal point, (f_1^*, f_2^*), maximizes both f_1 and f_2. A *Pareto curve* is a curve drawn through a locus of points between A and C that correspond to "non-dominated" function values. For example, point D is "dominated" with respect to f_1 and f_2 by all points on the dotted curve. We may use the curve to determine a best compromise design by choosing the point closest to the ideal point.

Figure 6 is a Pareto plot of test cases run with Re_D = 3980 at different pin fin spacings. Since minimizing the total pressure drop, Δp_t, is equivalent to maximizing $1/\Delta p_t$, both the passage heat flux, q'', and $1/\Delta p_t$ are objectives that are to be maximized. For consistency, the total pressure drop was computed using the same upstream and downstream locations relative to the pin location: five diameters upstream from the first row of fins, and eight diameters downstream from the last row. The total heat flux includes convection losses from all pin surfaces and the wall. The best candidate would be a point that maximizes q'' while maintaining high values for $1/\Delta p_t$. Note that for x/D = 2.25 to 4.0, $1/\Delta p_t$ values do not differ significantly. Of these points, x/D = 2.25 renders the highest heat flux, as shown in Table 1. Hence, we can conclude that x/D = 2.25 would be chosen as an optimum spacing for these flow conditions. To determine if x/D = 2.25 agrees with a more rigorous definition of "best compromise", we considered the expression,

$$\text{minimize } \max\left(\frac{f_1(\vec{x}) - f_1^*}{f_1^*}, \frac{f_2(\vec{x}) - f_2^*}{f_2^*}\right) \qquad (2)$$

where f_1^* represents the "best" f_1 value, and f_2^* represents the "best" f_2 value. Comparing the min-max values of each test

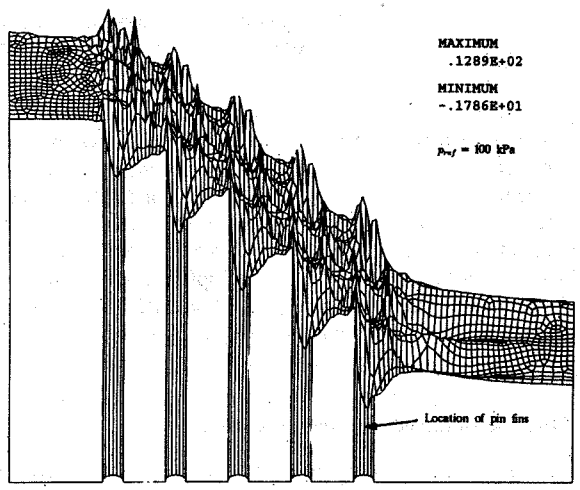

Figure 4: Surface total pressure plot with respect to p_{ref} for Re_D = 1270 and x/D = 1.5.

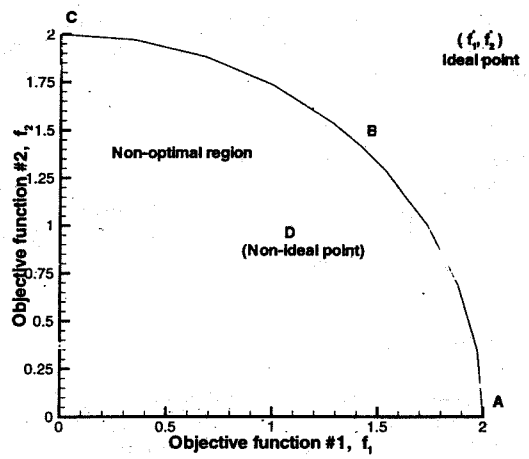

Figure 5: Generic Pareto curve.

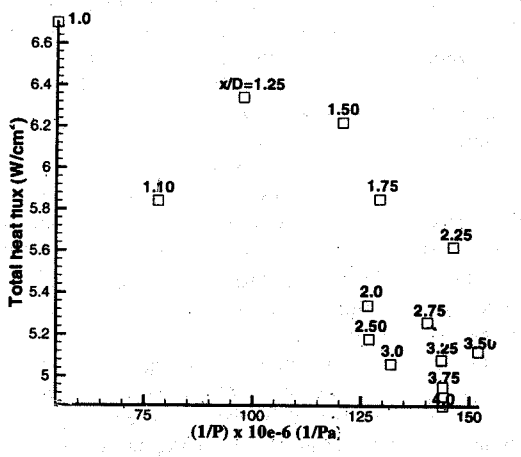

Figure 6: Pareto curve for Re_D = 3980.

case, the value of x/D = 2.25 rendered the lowest value of 0.01 (see Table 1). Thus, this would agree with the graphical solution depicted by figure 6.

Figure 7 combines the Pareto distributions for Re_D = 1270, 3980, 7310 and 13800. An optimum spacing is not so clear from looking at the pareto distribution for Re_D = 1270, but it would seem that x/D values between 2.0 and 4.0 are likely candidates. Computing the normalization for each case, x/D = 2.0 rendered the best solution (see Table 1). At Re_D = 7310 and Re_D = 13800, x/D = 1.75 were optimal (see figure 7). *Thus, longitudinal distances between 1.75 and 2.25 times the pin diameter can be starting grounds for designing pin fin arrangement that yield optimum cooling and pressure drop characteristics.*

Heat Flux Dependence on Row Location

Figure 8 shows the average heat flux from pins in each row with Re_D = 7310. There is an indication that maximum heat loss occurs with certain rows, where it appears to be row 4 for x/D = 4, and row 5 for x/D = 2. This can be attributed to the fact that flow through the passage behaves similarly to flow within a heat exchanger with a turbulence grid. Turbulence levels build up as flow moves downstream, and then levels off. It is here that the convection cooling can be expected to reach a maximum. *Such findings can be useful in determining the number of rows that would be sufficient for a particular passage.* Similar features were found at Re_D = 1270, 3980 and 13800. The number of possible designs and variables to examine is large, but this and future studies will provide useful information in determining optimum fin arrangements.

CONCLUSIONS

This study presents results from 2-D numerical simulations of coolant flow through a turbine blade cooling passage. The primary focus was to perform an optimization study to find x/D values that yielded high convection cooling while rendering minimal total pressure losses. The effects of one design parameter, the longitudinal pin spacing, x, were investigated by varying x while holding all other parameters constant (i.e., Re_D, T_i, D, and x_T). Fourteen values of (x/D) were investigated between 1.0 and 4.0 for four values of the Reynolds number: 1270, 3980, 7310, and 13800. It was found that for Re_D = 1270 an optimum spacing of x/D = 2.0 exists, while a slightly higher value of x/D = 2.25 is optimum for Re_D = 3980. For Re_D = 7310 and Re_D = 13800, x/D = 1.75 is optimum. There are also certain row locations for which the heat flux reaches a maximum. The heat flux reaches a maximum between rows 4 and 6 for the range of x/D values and Reynolds numbers studied. There are two competing effects that are responsible for heat flux values reaching a maximum. Moving through the pin fin array, the driving force for heat transfer, which is the difference between the averaged pin surface temperature and the coolant fluid temperature, decreases, thus the averaged heat flux would be forced to decrease. However, the turbulent kinetic energy is increasing up to row 6, which enhances convection cooling. Initially, the effect of increasing the turbulent kinetic energy dominates over the effect of a diminished temperature difference, and the net effect is for the averaged heat flux to increase. However, by rows 4 and

Set A					Set B				
Re_D = 1270, M_i = 0.024, U_i = 15.48m/s					Re_D = 3980, M_i = 0.076, U_i = 48.51m/s				
x/D	$q''(W/cm^2)$	T_o/T_i	$\Delta P_t(kPa)$	Min-max	x/D	$q''(W/cm^2)$	T_o/T_i	$\Delta P_t(kPa)$	Min-max
1.00	2.74	1.74	1.70	1.48	1.00	6.70	1.42	18.22	1.77
1.10	3.00	1.73	1.57	1.37	1.10	5.84	1.52	12.80	0.81
1.25	3.03	1.68	1.05	0.59	1.25	6.34	1.50	18.24	0.51
1.50	2.80	1.62	0.83	0.18	1.50	6.22	1.52	8.30	0.19
1.75	2.58	1.62	0.81	0.13	1.75	5.85	1.53	7.74	0.05
2.00	2.67	1.60	0.71	0.04	2.00	5.34	1.53	7.90	0.19
2.25	2.55	1.60	0.71	0.08	2.25	5.62	1.56	6.84	0.01
2.50	2.59	1.60	0.66	0.14	2.50	5.18	1.54	7.88	0.03
2.75	2.44	1.61	0.71	0.12	2.75	5.26	1.53	7.13	0.13
3.00	2.43	1.60	0.67	0.18	3.00	5.06	1.54	7.58	0.10
3.25	2.31	1.64	0.70	0.18	3.25	5.08	1.53	6.96	0.18
3.50	2.27	1.60	0.68	0.22	3.50	5.12	1.56	6.58	0.24
3.75	2.25	1.62	0.70	0.20	3.75	4.95	1.54	6.95	0.20
4.00	2.21	1.63	0.69	0.23	4.00	4.86	1.54	6.95	0.22
Set C					Set D				
Re_D = 7310, M_i = 0.140, U_i = 89.10m/s					Re_D = 13800, M_i = 0.265, U_i = 168.20m/s				
x/D	$q''(W/cm^2)$	T_o/T_i	$\Delta P_t(kPa)$	Min-max	x/D	$q''(W/cm^2)$	T_o/T_i	$\Delta P_t(kPa)$	Min-max
1.00	11.0	1.48	58.46	2.02	1.00	18.81	1.52	200.45	2.28
1.10	9.03	1.48	39.52	0.86	1.10	16.14	1.61	132.49	1.03
1.25	9.67	1.56	31.00	0.48	1.25	15.94	1.63	102.90	0.53
1.50	9.18	1.61	25.55	0.16	1.50	15.05	1.69	83.68	0.17
1.75	8.75	1.63	23.37	0.01	1.75	14.21	1.70	76.30	0.01
2.00	8.37	1.62	24.31	0.02	2.00	14.07	1.68	79.60	0.05
2.25	8.31	1.67	20.22	0.02	2.25	13.53	1.75	65.77	0.20
2.50	8.04	1.62	24.17	0.02	2.50	13.45	1.68	80.44	0.03
2.75	7.95	1.62	20.94	0.20	2.75	13.09	1.72	67.14	0.21
3.00	7.87	1.63	25.55	0.04	3.00	13.08	1.71	75.32	0.07
3.25	7.58	1.63	23.36	0.10	3.25	12.30	1.72	67.05	0.25
3.50	7.62	1.67	19.34	0.31	3.50	11.94	1.75	61.14	0.36
3.75	7.37	1.64	20.68	0.26	3.75	11.88	1.73	65.96	0.29
4.00	7.24	1.65	20.58	0.28	4.00	11.73	1.73	66.46	0.29

Table 1: Flow Passage Test Cases and Results.

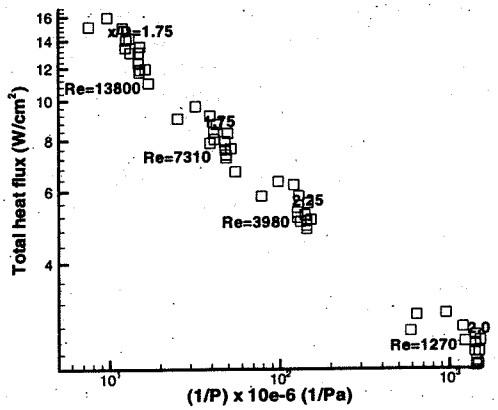

Figure 7: Pareto distributions for entire range of Reynolds numbers studied.

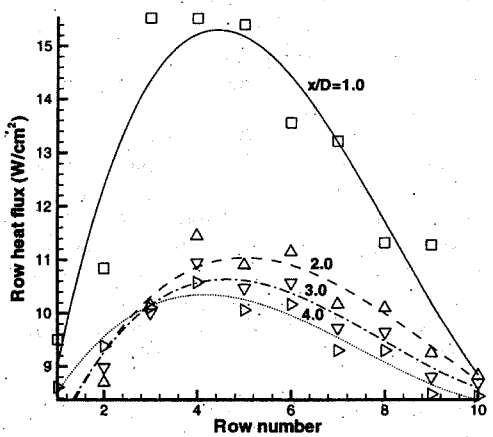

Figure 8. Heat Flux vs Row Number for Re = 7310.

5, increases in the turbulent kinetic energy become negligible, eventually leveling off, and the effect of a continually decreasing temperature difference becomes dominant, thus lowering the averaged heat flux values. These findings apply only to circular fins in a staggered alignment, but can serve as a baseline for which subsequent designs can be made.

ACKNOWLEDGEMENTS

The authors would like to thank the National Science Foundation Graduate Research Traineeship (NSF-GRT) Program in Environmentally Conscious Manufacturing at The Pennsylvania State University for partially funding this research and the Center for Academic Computing for the computing time made available.

References

[1] Y. Peng. *Heat Transfer and Friction Characteristics of Pin Fin Cooling Configuration.* ASME Journal of Heat Transfer, 83, 1-6, 1983.

[2] Armstrong, J. and Winstanley, D. *A Review of Staggered Array Pin Fin Heat Transfer for Turbine Cooling Applications.* ASME Journal of Heat Transfer, 110, 94-103, 1988.

[3] Metzger, D.E. and Haley, S.W. *Heat Transfer Experiments and Flow Visualization for Arrays of Short Pin Fins.* ASME Paper No. 82-GT-138, 1982.

[4] Metzger, D.E. and Haley, S.W. *Effects of Pin Shape and Array Orientation on Heat Transfer and Pressure Loss in Pin Fin Arrays.* Journal of Engineering for Gas Turbine and Power, 106, 252-257, 1984.

[5] Metzger, D.E. and Shepard, W.B. *Row-Resolved Heat Transfer Variations in Pin Fin Arrays Including Effects of Non-Uniform Arrays and Flow Convergence.* ASME Paper No. 86-GT-132, 1986.

[6] VanFossen, G.J. *Heat Transfer Coefficients for Staggered Arrays of Short Pin Fins.* ASME Journal of Engineering for Power, 104, 268-274, 1981.

[7] VanFossen, G.J. *Heat Transfer Coefficient for Staggered Arrays of Short Pin Fins.* Journal of Engineering for Power, 104, 268-274, 1984.

[8] Chyu, M.K. *heat Transfer and Pressure Drop for Short Pin-Fin Arrays with Pin Endwall.* Journal of Heat Transfer, 112, 926-932, 1990.

[9] Chyu, M.K., Hsing, Y.C., and Natarajan, V. *Convective Heat Transfer of Cubic Fin Arrays in a Narrow Channel.* ASME Paper No. 96-GT-201, 1996.

[10] *FIDAP 7.0 Tutorial Manual* Fluid Dynamics International, Inc., Chp 7, 1993.

[11] Brigham, B.A. and VanFossen, G.J. *Length-to-Diameter Ratio and Row Number Effects in Short Pin Fin Heat Transfer.* ASME Journal of Engineering for Gas Turbines and Power, Vol. 106, 1987, pp 241-245.

[12] Panton, Ronald L. *Incompressible Flow.* John Wiley and Sons, Inc., 1984, pp 334-338.

[13] Sparrow, E.M., Ramsey, J.M., and Altemani, C.A.C. *Experiments on In-Line Pin Fin Arrays and Performance Comparisons with Staggered Arrays.* ASME Journal of Heat Transfer, Vol.102, pp 44-50.

[14] Zhang, Y.M., Han, J.C. and Parsons, J.A. *Surface Heating Effect on Local Heat Transfer In a Rotating Two-Pass Square Channel With 60 Degree Angled Rib Turbulators.* ASME Paper No. 93-GT-336, 1993, pp 1-9.

[15] Zukaukas, A.A. *Heat Transfer From Tubes in Cross Flow* Adv. in Heat Transfer, Vol. 8, pp 116-133.